A New Model of Magnetic Force in Magnetic Levitation Systems

Y. S. Lee†, J. H. Yang* and S. Y. Shim*

Abstract – In this paper, we propose a new model of the magnetic control force exerted on the levitation object in magnetic levitation systems. The model assumes that the magnetic force is a function of the voltage applied to an electromagnet and the position of a levitation object. The function is not explicitly expressed but represented through a 2D lookup table constructed from the experimentally measured data. Unlike the conventional model that reveals only local characteristics of the magnetic force, the proposed model shows global characteristics satisfactorily. Specially devised measurement equipment is utilized in order to gather the data required for model construction. An experimental procedure to construct the model is presented. We apply the proposed model to designing a sliding mode controller for a lab-built magnetic system. The validity of the proposed model is illustrated by comparing the performances of the controller adopting the conventional model with that of the controller adopting the proposed model.

Keywords: 2D Lookup table; Magnetic force; Magnetic Levitation System; Sliding Mode Control

1. Introduction

Magnetic levitation systems have practical importance in many engineering systems such as high-speed maglev passenger trains, frictionless bearings, levitation of wind tunnel models, etc. [7-10]. They have been used for educational purposes in teaching students on the concept of feedback control. A lot of studies have been conducted for the control of magnetic levitation systems. In order to handle nonlinear characteristics of the systems, various nonlinear control techniques such as sliding mode control, feedback linearization, and backstepping have been applied [2, 6, 9]. When applying model-based control, accurate system modeling needs to precede designing of a controller. In particular, the magnetic force exerted on the levitation object should be carefully characterized for good control of magnetic levitation systems.

Magnetic control force exerted on the levitation object is a function of the coil current and the displacement between the levitation object and the electromagnet. The effect of the coil current on the magnetic control force exerted on the levitation object at a certain position differs depending on the substance of the levitation object. If the levitation object is a ferromagnetic ball, the magnetic force is proportional to the square of the coil current [5, 6, 11, 13, 15]. If the levitation object is a permanent magnet, the magnetic force is proportional to the coil current [3]. In [2], where the levitation object is a permanent magnet, it is assumed that the magnetic force is proportional to the voltage applied to the electromagnet. Analytical expression of the exerted magnetic force due to the object's position is very complex and nonlinear. Refer to the analytical expression derived in [6] for example. Such a complex expression is not preferred in designing controllers for magnetic levitation systems. Therefore, in existing literatures dealing with the control of magnetic levitation systems, simplified or experimentally calibrated characteristics on magnetic force are preferred. In [1, 5, 11, 13, 15], it is assumed for simplicity that the magnetic force is inversely proportional to the square of the sum of the displacement of the levitation object and a system-dependent constant. In [2, 3, 6], the magnetic force is characterized such that it is inversely proportional to a polynomial function on the displacement of the levitation object. The polynomial function is obtained through experimental calibration including least square fitting. The calibration approach is somewhat heuristic but well characterizes the magnetic force. However, it should be mentioned that the obtained characteristics are only local in a sense that it works good when the mass of the levitation object is around a certain value. This is because the experimental data used for the calibration of the polynomial function is obtained with respect to a levitation object of specific mass. Furthermore, the

† Corresponding author. This work was supported by KESRI (R-2007-2-059), which is funded by MOCIE (Ministry of Commerce, Industry, and Energy). (e-mail: lys@inha.ac.kr, {zero1zuck, syong82}@hanmail.net)
* School of Electrical Engineering, Inha University, 253 Yonghyundong, Inchon, Korea.
Received 28 March 2008 ; Accepted 5 August 2008

experiment takes a lot of time because it requires repetitive actions and continuous human attention to catch the values needed for calibration.

In this paper, we propose an improved model for magnetic force exerted on the levitation object. The proposed model removes two main drawbacks of the exiting calibration-based models: locality, and tedious experimental procedure. We do not restrict the model to any prescribed functional form unlike the existing models. The function is not explicitly expressed. Instead, we utilize a 2D lookup table to represent the function numerically. In addition, we propose specially devised measurement equipment, which speeds up the experimental procedure. Modeling automation will be possible with a slight modification to the equipment. The validity of the proposed model is illustrated by comparing the performance of a controller adopting the proposed model with that of a controller adopting the existing model.

The rest of the paper is organized as follows: Section 2 introduces an experimental prototype of a magnetic levitation system and defines a problem statement to be considered in the paper. In Section 3, we propose a new model and modeling method using specially devised measurement equipment. In Section 4, we design sliding mode control adopting the proposed model and give experimental results for illustration. Finally in Section 5, we make conclusions.

2. Experimental Prototype and Problem Statement

A schematic diagram of the magnetic levitation system used in the experiment is shown in Fig. 1. The levitation object is a cylindrical aluminum block with a strong magnet embedded on top of it, as shown in Fig. 2. An infrared (IR) emitter and phototransistors are used to determine the position of the levitation object. Five phototransistors are used in order to make a wide sensing range available. Voltage outputs from five phototransistors are fed to a signal conditioning circuit depicted in Fig. 3. The circuit yields a single voltage output, V_s, which is converted to digital data through a 12-bit AD converter. A computer-based controller computes the control using the digital position information at a sample rate of 1 kHz. Magnetic control force is generated from a lab-built electromagnet by adjusting the voltage applied to the electromagnet according to the computed control.

Using the fundamental principle of dynamics, the dynamic equation of the magnetic levitation system is given by

$$\ddot{x} = g - \frac{F}{m}, \tag{1}$$

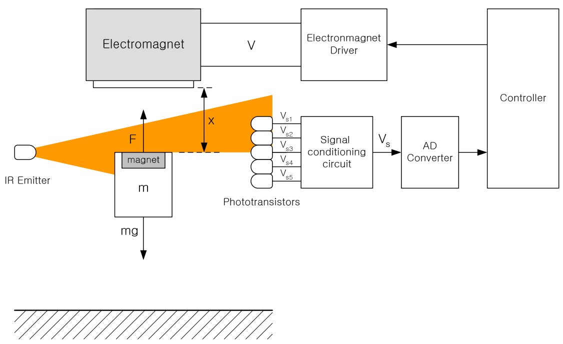

Fig. 1. Schematic diagram of a magnetic levitation system

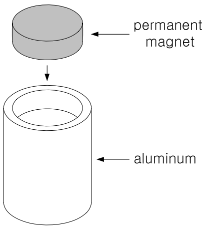

Fig. 2. Levitation object with a permanent magnet attached

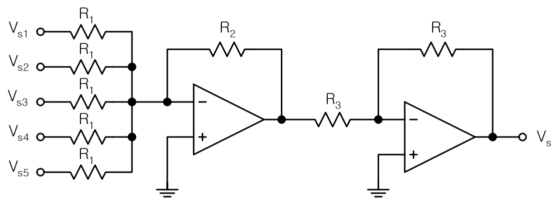

Fig. 3. Signal conditioning circuit

Table 1. Existing models of the magnetic force

Reference	[2]	[3]	[6]
Levitation object	Permanent magnet	Permanent magnet	Ferromagnetic ball
Model function	$F = \frac{V}{a(x)}$	$F = \frac{i}{a(x)}$	$F = \frac{i^2}{a(x)}$

where m is the mass of the levitation object, x is the displacement from the top of the levitation object to the bottom of the electromagnet, g is the gravitational constant, and F is the magnetic force exerted on the levitation object by the electromagnet. A positive value of F implies attracting force and negative value repelling force. One may want to find the analytical expression of the magnetic force exerted on the levitation object by considering the magnetic field, as considered in [6]. However, the analytical expression of the magnetic force is very complex for the lab-built experimental apparatus, as mentioned in [2, 6]. Therefore, in some existing studies, the magnetic force characteristics are experimentally calibrated as functions of the position of the levitation object and the electrical value (voltage or current). Table 1 compares the model functions of the magnetic force used in the existing studies, where $a(x)$ is a polynomial function of x, that is, $a(x)=a_0+a_1x+\cdots+a_nx^n$. n is the order of the polynomial function and a_0 to a_n are the coefficients of the polynomial function to be determined experimentally. The experiment performed to find the coefficients consists of determining the minimum voltage (or current) to pick up the levitation object of mass m at various positions. The force required to pick up the levitation object of mass m is mg [N]. Therefore, we can write

$$F = mg = \frac{V(\text{or } i \text{ or } i^2)}{a_0 + a_1x + a_2x^2 + \cdots + a_nx^n},$$

which can be rewritten into

$$\frac{V(\text{or } i \text{ or } i^2)}{mg} = a_0 + a_1x + a_2x^2 + \cdots + a_nx^n. \qquad (2)$$

The data are then least-squares fitted to determine the order and the coefficients of the polynomial function. Fig. 4 depicts the control block diagram in which a conventional model adopted in [2] is utilized. Since the voltage to the electromagnet can be manipulated, the control force obtained through the control algorithm is converted to the voltage required to generate that force using the relation $V = a(x)F$. In case of [3, 6], the current required to generate the magnetic force is obtained using the inverse relations. The obtained current is actually generated by a high-bandwidth current loop.

It should be mentioned that existing models and modeling methods have two drawbacks. Firstly, the controller designed using the existing models are not robust against the mass variation of the levitation object. This is because the coefficients of the polynomial function, $a(x)$, are dependent on the mass of the levitation object used in the calibration experiment. The model obtained through existing methods is valid only when the actual mass of the levitation object is near the value used in the calibration experiment. Hence, if one tries to levitate an object the mass of which is much different from the one used in the calibration experiment, the controller is very likely to show poor performance or even worse to destabilize the system. Secondly, the experimental procedure is not appropriate for automation because one should keep an eye on the levitation object in order to catch the moment when the object is picked up.

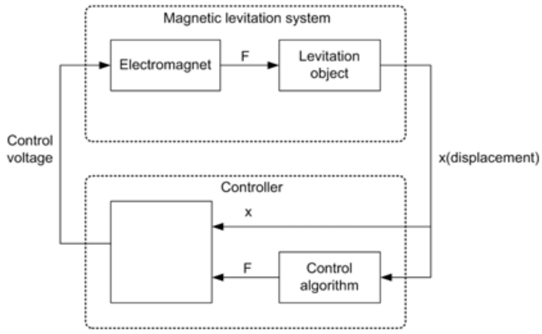

Fig. 4. Control block diagram using the conventional magnetic force model

The purpose of this paper is to propose a new model of the magnetic force in magnetic levitation systems and a new modeling method. The proposed method greatly removes the drawbacks of the existing methods, which will be well illustrated through experiments later in the paper. In the next section, we propose a new model and modeling method. We also introduce lab-built measurement equipment that is used in the modeling procedure.

3. New Model and Modeling Method

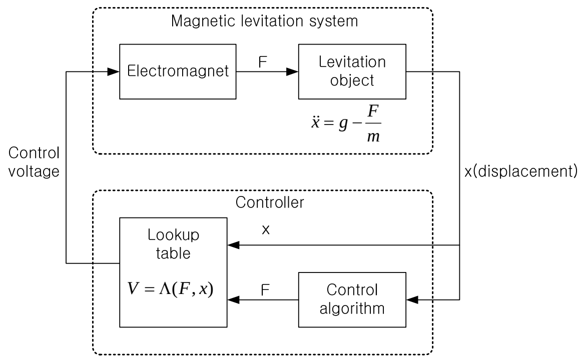

Fig. 5. Control block diagram using the proposed magnetic force model

Table 2. Meaning of part symbols

Symbol	Meaning
a	rotating handle
b	linear motion shaft
c	lead screw
d	mount table
e	load cell
f	mount table for position sensor modeling
g	incremental rotary encoder
h	screw nut
i	linear bushing
j	adaptor for attaching a load cell

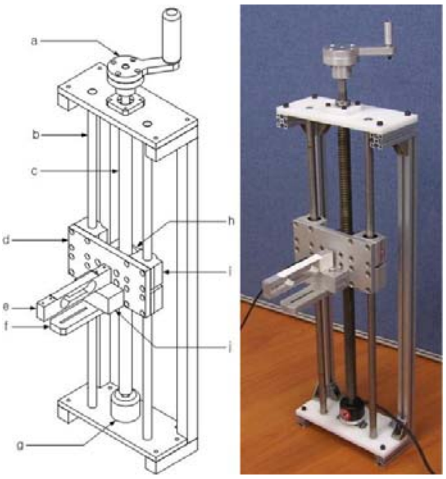

Fig. 6. Lab-built measurement equipment: schematic diagram (left) and picture (right)

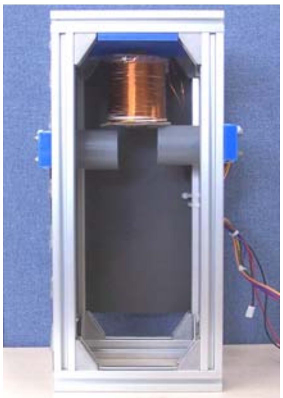

Fig. 7. A Lab-built magnetic levitation system

As mentioned in the previous section, the conventional model is effective only when the mass of the levitation object is near the mass of the object used in the calibration procedure. In this section, we propose a new model, described by the function $F = \sum(V,x)$, in order to remove the drawback of the conventional model. The function $F = \sum(V,x)$ maps the magnitude of the magnetic force exerted on the object located at displacement x, when the voltage input to the electromagnet is V volts. It is noted that the proposed model $F = \sum(V,x)$ reveals global characteristics of the magnetic force. We can also think of the function $V = \Lambda(F,x)$, which maps the voltage input required for the electromagnet to exert the magnetic force F on the levitation object located at displacement x. Analytic representation of $F = \sum(V,x)$ and $V = \Lambda(F,x)$ is hardly available for lab-built electromagnets and thus the approach taken in this paper is to represent those functions using a 2D lookup table constructed from measured experimental data.

Fig. 5 depicts the control block diagram using the proposed model of the magnetic force. The control algorithm computes the required magnetic force based on displacement x. The computed magnetic force F is fed to a 2D lookup table, which is a numerical representation of $V = \Lambda(F,x)$, in order to find the voltage input to the electromagnet required to generate the force in reality. Since the model describes the global characteristics of the magnetic force better, it is natural to expect that the resulting control performances are better. The question is how to obtain the relation $F = \sum(V,x)$ and $V = \Lambda(F,x)$. For this purpose, we utilize specially devised measurement equipment. Fig. 6 shows the schematic diagram and real picture of the equipment. Table 2 explains the meaning of the part symbols given in Fig. 6.

For convenience of explanation, we use symbols surrounded by parentheses in order to indicate parts in the equipment. The lead screw (c) converts rotary motion of the rotating handle to linear motion of the mount table (d). The advance per revolution of the lead screw used in the equipment is 4 [mm]. A rotary encoder (g) is installed at the end of the lead screw in order to measure the angular displacement. It generates 4000 pulses per revolution. Therefore, the linear motion of the mount table can be measured at 1 [μm] resolution. A small mount table (f) can be attached to the table (d) at right angle for position sensor modeling. A load cell (e) can also be attached to the mount table using an adaptor block (j). A load cell is an electronic transducer that is used to convert a force into a measurable electrical output. The load cell used in this paper has the measurement range of 3 Kg. A lab-built magnetic levitation system shown in Fig. 7 is utilized as a target to which the proposed modeling method is to be applied.

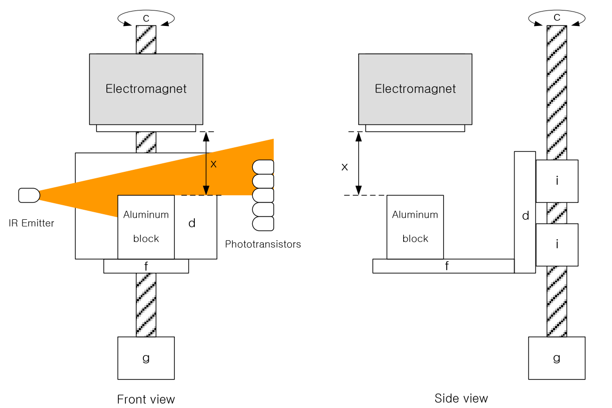

Fig. 8. Conceptual diagram for position sensor modeling experiment

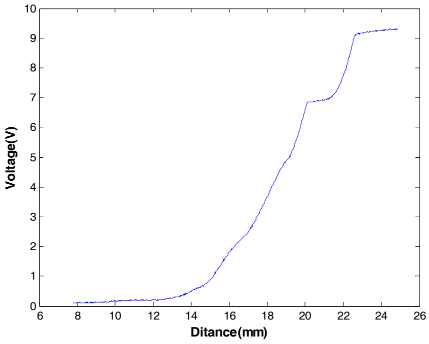

Fig. 9. Experimentally obtained relation x and V_S

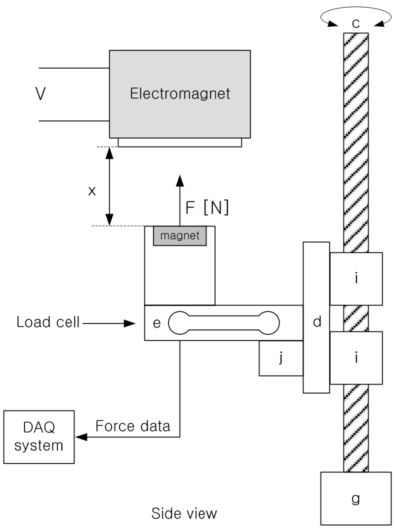

Fig. 10. Conceptual diagram for magnetic force modeling experiment

Before we model the magnetic force, we model the characteristics of the position sensor implemented in combination of an IR emitter and phototransistors (see Fig. 1). Fig. 8 describes the conceptual diagram of the experimental setup for position sensor modeling. We detach a load cell (e) and adaptor block (j) from the mount table (d). We fix an aluminum block on top of the small mount table (f) such that it can block infrared rays emitted from the IR emitter. The experimental procedure for position sensor modeling is as follows:

Step 1. Move up the mount table by adjusting the rotating handle until the aluminum block hits the bottom of the electromagnet. Then, set $x = 0$.

Step 2. Lower the mount table by adjusting the rotating handle and save the displacement data and V_S.

The electromagnet is not activated at this experiment. Instead, the IR emitter and phototransistors should be turned on. The displacement data can be obtained from the rotary encoder. Sensor voltage output is obtained at the end of a signal conditioning circuit (See Fig. 3). Fig. 9 shows the experimentally obtained relation between displacement x and corresponding sensor voltage output V_S. Since the phototransistors are not ideally installed, the resulting relation is not smooth. If the relation is represented in a smooth curve, a polynomial approximation method may be used as in [2] in order to model sensor characteristics. It is observed that the relation corresponding to $14[\text{mm}] \le x \le 20[\text{mm}]$ is represented in a smooth curve. However, the global relation is not represented in a smooth curve and thus a polynomial approximation method is not appropriate in our case. Instead, we choose to represent the relation given in Fig. 9 through a 1D lookup table. Now we can retrieve the absolute position of the levitation object using the voltage output of the position sensor.

Then we are ready to perform the experiment for magnetic force modeling. Fig. 10 depicts the conceptual diagram of the experimental setup. For this experiment, the load cell (e) is attached to the mount table (d) using the adaptor block (j). A levitation object given in Fig. 2 is fixed to the load cell (e) using bolts. We assume that the displacement and voltage applied to the electromagnet has the following range:

$$x_{\min} \le x \le x_{\max}, \quad V_{\min} \le V \le V_{\max}.$$

The range limitation on the displacement x comes from the fact that validity of the position sensor is limited to a certain range. We propose the following experimental procedure for magnetic force modeling:

Step 1. Set the applied voltage $V = V_{\min}$.

Step 2. Lower the levitation object to $x_{\max}$.

Step 3. Move the levitation object slowly from $x_{\max}$ to $x_{\min}$ and save the measured force and displacement data.

Step 4. Set the applied voltage $V = V + \delta V$.

Step 5. Check whether $V > V_{\max}$. If yes, stop. If not, go to Step 2.

Force data is measured through the load cell and the displacement data is retrieved from the 1D lookup table constructed from the procedure mentioned above. Fig. 11 indicates a 3D plot drawn from the data gathered through the experimental procedure mentioned above. We chose $x_{\min} = 14$ [mm], $x_{\max} = 22$ [mm], $\delta = 0.5$ [volt], $V_{\min} = 0$ [volt], and $V_{\max} = 25$ [volt]. The function $V = \Lambda(F, x)$ can be approximately constructed from the data presented in Fig. 11 using interpolation. Fig. 12 shows the mapping relation of $V = \Lambda(F, x)$ using a 3D plot. The flat surface in Fig. 12 is due to the voltage saturation at 25 volts.

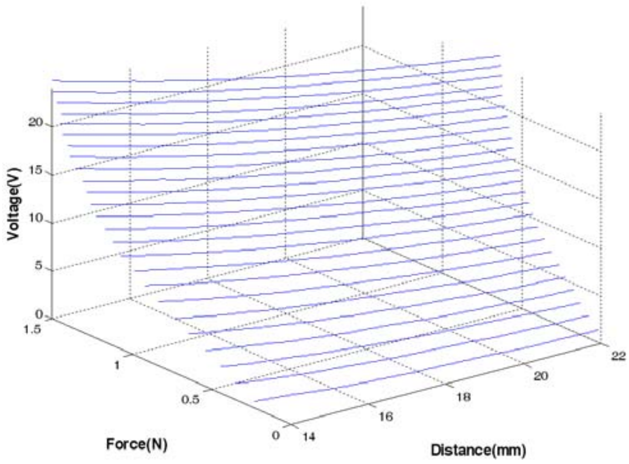

Fig. 11. Data obtained through the proposed modeling method

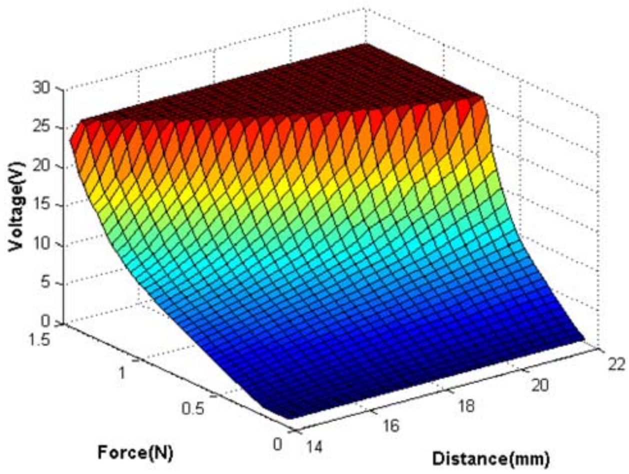

Fig. 12. Experimentally obtained magnetic force model, $V = \Lambda(F, x)$.

Remark 3.1. We can assume $F = \sum(i, x)$ and $i = \Lambda(F, x)$. The proposed modeling method can also be applied to obtain that relation. For this experiment, we need an additional current sensor. We chose $F = \sum(V, x)$ and $V = \Lambda(F, x)$ for simplicity.

Remark 3.2. Because we use a load cell to measure the force, continuous human attention required in conventional modeling procedure is not necessary in the proposed modeling procedure. If we use a motor to rotate the lead screw in the measurement equipment, the experimental procedure given above can be made fully automated by an appropriate programming. As a result, the proposed modeling method removes the tedious procedure in the conventional modeling method.

4. Controller Design and Experimental Results

In this section, we design a controller for our lab-built magnetic levitation system and apply two magnetic force models, i.e., conventional model and proposed model, in order to show the validity of the proposed model through comparison. We chose to use sliding mode control among various control methods. Sliding mode control is a well-known control method for nonlinear systems [12, 14]. We adopt the control structure taken in [2]. Let us define the position reference to be x_d. Then, the tracking error is given by

$$e(t) = x - x_d .$$

Choose the sliding surface as follows:

$$S(t) = \dot{e}(t) + c_1 e(t) + c_2 \int_0^t e(\tau) d\tau,$$

where $c_1 > 0$ and $c_2 > 0$ are design parameters. As widely known, the attraction condition of the $S(t) = 0$ manifold is:

$$S(t)\dot{S}(t) < 0 .$$

The above attraction condition is satisfied by selecting the control input such that $\dot{S}(t) = -\eta \operatorname{sign}(S(t))$, where $\eta > 0$ is a design parameter. The time derivative of $S(t)$ is

$$\begin{aligned}\dot{S}(t) &= \ddot{e}(t) + c_1 \dot{e}(t) + c_2 e(t) \\ &= \ddot{x} - \ddot{x}_d + c_1 \dot{e}(t) + c_2 e(t) \\ &= g - \frac{F}{m} - \ddot{x}_d + c_1 \dot{e}(t) + c_2 e(t).\end{aligned}$$

Let's take F as follows:

$$F = m_c[g - \ddot{x}_d + c_1 \dot{e} + c_2 e + \eta \operatorname{sign}(S(t))],$$

where m_c is the mass of the object that the control intends to levitate. If $m = m_c$, where m is the actual mass of the levitation object, then $S(t)\dot{S}(t) = -\eta\,|\,S(t)\,| < 0$ for $S(t) \neq 0$. This implies that manipulating the electromagnet such that it exerts the magnetic force given by (3) on the levitation object makes the tracking error e approach zero as time passes. Since we can manipulate the voltage applied to the electromagnet, the control law should be represented in terms of voltage input to the electromagnet.

Suppose that we use the conventional magnetic force model, i.e., $F = V / a(x)$. The control law is represented as follows:

$$V = a(x)m_c[g - \ddot{x}_d + c_1\dot{e} + c_2 e + \eta \mathrm{sign}(S(t))]. \qquad (4)$$

On the other hand, the proposed magnetic force model is represented by $V = \Lambda(F, x)$. Therefore, the control law adopting the proposed model is represented as follows:

$$V = \Lambda(m_c[g - \ddot{x}_d + c_1\dot{e} + c_2 e + \eta \mathrm{sign}(S(t))],\ x). \qquad (5)$$

As already mentioned, $\Lambda(\cdot,\cdot)$ is represented using a 2D lookup table. In order to alleviate the chattering problem inherent in sliding mode control, $\mathrm{sign}(S(t))$ function can be replaced by $\mathrm{sat}(S(t))$ defined as follows:

$$\mathrm{sat}(S(t)/\phi) = \begin{cases} sign(S(t)) & ,\ if\ \ |\,S(t)\,| \geq \phi \\ S(t)/\phi & ,\ if\ \ |\,S(t)\,| < \phi \end{cases}$$

where $\phi > 0$ is a design parameter.

Remark 4.1. Assume that $m \neq m_c$, which implies that there exists uncertainty in mass. Then $S(t)\dot{S}(t) < 0$ may not hold, which implies the stability is not guaranteed. Because the controller from (4) and (5) both include the term m_c, both controllers can suffer from degradation of the control performance due to the mass uncertainty. However, the control form adopting the conventional model is more vulnerable to performance degradation because $a(x)$ can closely characterize the magnetic force when the actual mass of the levitation object is close to the mass of the object used in the calibration experiment. On the other hand, $\Lambda(\cdot,\cdot)$ globally characterizes the magnetic force. As a result, it is expected that the control given by (5) is more robust against the variation in the mass of the levitation object, which will be shown through experiments later in the paper.

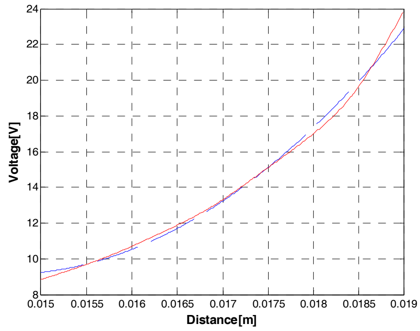

Fig. 13. Model comparison for $m = 90\,[g]$ (dotted: conventional, solid: proposed)

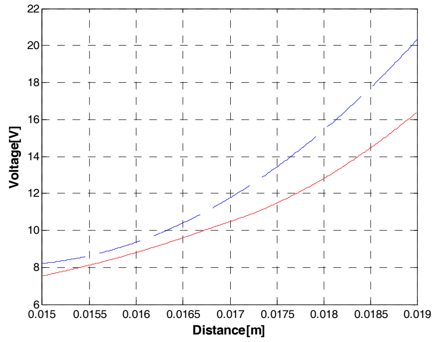

Fig. 14. Model comparison for $m = 80\,[g]$ (dotted: conventional, solid: proposed)

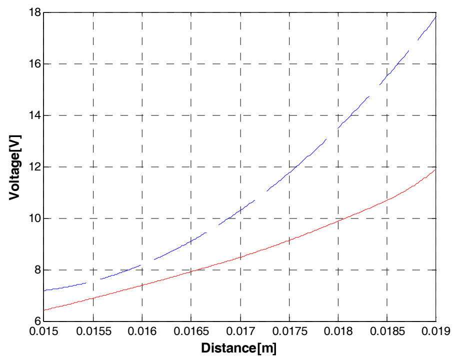

Fig. 15. Model comparison for $m = 70\,[g]$ (dotted: conventional, solid: proposed)

In order to show the validity of the proposed model, we compare the performance of a controller adopting the proposed model with that of a controller adopting a conventional model. The polynomial $a(x)$ for the conventional model is obtained through calibration experiment using the object with $m = 90\,[g]$. $a(x)$ is obtained as follows:

$$a(x) = 630590x^2 - 17529x + 130.91.$$

Since the conventional model assumes $V = a(x)F$, the voltage required to levitate the object with mass $m\,[g]$ at the displacement of x is computed as follows:

$$V = a(x) \times m \times 0.001 \times 9.8.$$

However, the above relation is valid only when we levitate the object with $m = 90\,[g]$. If we levitate the object of different mass, the above relation will yield the voltage inappropriate for levitating that object. Closed loop control may mitigate the bad effect due to this model inaccuracy. However, it is naturally expected that the control performance will deteriorate. Figs. 13 and 14 compare relations on voltage vs. displacement obtained from the conventional model and the proposed model, respectively, for three different cases of mass. In case of $m = 90\,[g]$, both models reveal similar characteristics (See Fig. 13). However, the characteristics of the conventional model differ much from those of the proposed model when $m \neq 90\,[g]$ (See Fig. 14 and Fig. 15). These clearly show that the conventional model only catches the local characteristics of the magnetic force in a sense that it is effective only when the levitation object has specific mass. Let us move on to real control experiments.

In order to compare the control performances, we used three levitation objects with $m = 90\,[g]$, $m = 80\,[g]$, and $m = 70\,[g]$. Because $a(x)$ is obtained assuming $m = 90\,[g]$, we set $m_c = 90\,[g]$ for controller design. Firstly, we used the levitation object with $m = 90\,[g]$. Since $m_c = 90\,[g]$, there is no uncertainty in mass. The tracking responses of the controller adopting two different models are compared in Fig. 16. It is observed that there is little difference in the tracking responses. This little difference is well expected because $a(x)$ is obtained using the object with $m = 90\,[g]$. Therefore, the conventional model also well characterizes the magnetic force. Secondly, we used the levitation object with $m = 80\,[g]$. Fig. 17 compares the tracking responses of both controllers. It is seen that the controller adopting the conventional model exhibits oscillatory response. On the other hand, the controller adopting the proposed model maintains good tracking response despite the mass uncertainty. Finally, we used the levitation object with $m = 70\,[g]$ and Fig. 16 compares the tracking responses. It is seen that the controller adopting the conventional model diverges. On the other hand, the controller adopting the proposed model still maintains acceptable tracking response. These three experiments clearly show that the proposed model characterizes the magnetic force more closely than the conventional model. The resultant controller is shown to be more robust against the variation in the mass of the levitation object.

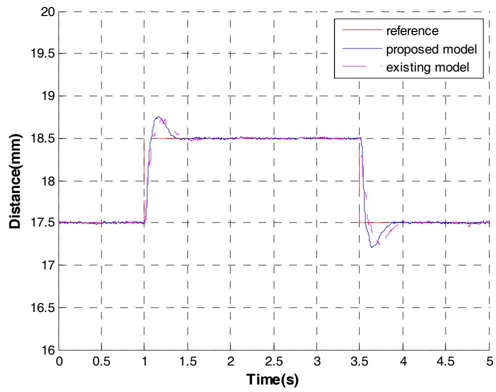

Fig. 16. Tracking response comparison. ($m_c = m = 90\,[g]$).

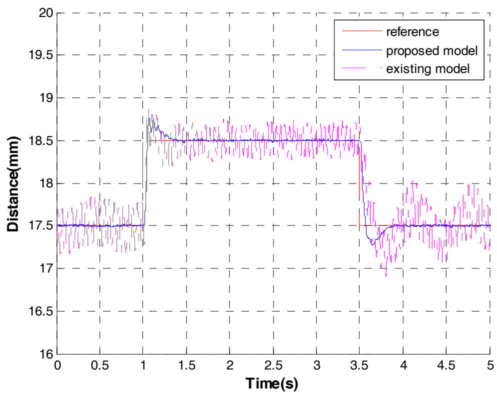

Fig. 17. Tracking response comparison. ($m_c = 90\,[g]$, $m = 80[g]$).

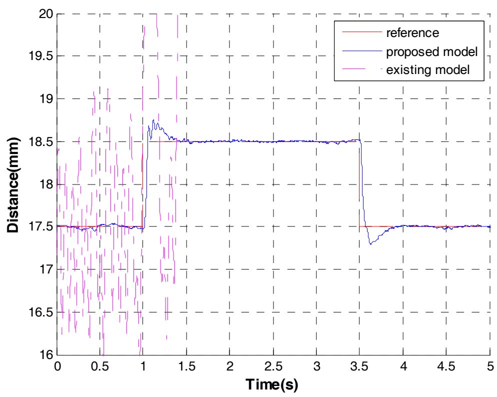

Fig. 18. Tracking response comparison. ($m_c = 90\,[g]$, $m = 70[g]$).

5. Conclusions

In this paper, we proposed a new model of the magnetic control force in magnetic levitation systems. The new model is represented numerically using a 2D lookup table. Unlike the conventional model that reveals the local characteristics only, the proposed model has a feature that it shows the global characteristics of the magnetic force satisfactorily. In order to construct the proposed model through experiments, we specially devised new measurement equipment. An experimental procedure to construct the model using the equipment was presented. The proposed procedure removes the drawbacks of the existing experimental procedures. For illustration of the validity of the proposed model, we applied it in designing a sliding mode controller for a lab-built magnetic system. The controller based on the proposed model was shown to be more robust against mass variation than the controller adopting the conventional model.

References

[1] N.F. Al-Muthairi and M. Zribi, "Sliding control of a magnetic levitation system," *Mathematical Problems in Engineering*, Vol. 2, pp. 93-104, 2004.

[2] D. Cho, Y. Kato and D. Spilman., "Sliding mode and classical control magnetic levitations systems," *IEEE Control Systems Magazine*, Vol. 13, pp. 42-48, 1993.

[3] J.S. Choi and Y.S. Baek, "A single DOF magnetic levitation system using time delay control and reduced-order observer," *KSME International Journal*, Vol. 16, No. 12, pp. 1643-1651, 2002.

[4] M. Dussaux, "The industrial applications of the active magnetic bearings technology," *Proceedings of the 2nd Int. Symp. Magnetic Bearings*, pp. 33-38, 1990.

[5] M. Fujita and T. Namerikawa, "μ-Synthesis of an electromagnetic suspension systems," *IEEE Transactions on Automatic Control*, Vol. 40, No. 3, pp. 530-536, 1995.

[6] A.E. Hajjaji and M Ouladsine, "Modeling and nonlinear control of magnetic levitation systems," *IEEE Transactions on Industrial Electronics*, Vol. 48, No. 4, pp. 831-838, 2001.

[7] B.Z. Kaplan and D. Redev, "Dynamic stabilization of tuned-circuit levitators," *IEEE Transactions on Magnetics*, Vol. Mag-12, pp. 556-559, 1976.

[8] D.A. Limbert, H.H. Richardson and D.N. Wormley, "Controlled characteristics of ferromagnetic vehicle suspension providing simultaneous lift and guidance," *Trans. ASME, J. Dyn. Syst. Meas. Control*, Vol. 101, pp. 217-222, 1990.

[9] F.J. Lin, L.T. Teng, and P.H. Sheh, "Intelligent Adaptive Backstepping Control System for Magnetic Levitation Apparatus," *IEEE Transactions on Magnetics*, Vol. 43, No. 5, pp. 2009-2018, 2007.

[10] J.E. Pad, "State variable constraints on the performance of optimal Maglev suspension controllers," *Proceedings of IEEE Conf. Control Applications*, pp. 124-127, 1994.

[11] P.S. Shiakolas, S.R. Van Schenck, D. Piyabongkarn and I. Frangeskou, "Magnetic levitation hardware-in-the-loop and MATLAB-based experiment for reinforcement of neural network control concepts," *IEEE Trans. Edu.*, Vol. 47, pp. 33-41, 2004.

[12] J.E. Slotine and W. Li, *Applied Nonlinear Control*, Prentice-Hall, 1991.

[13] D.L. Trumper, "Linearizing control of magnetic suspension systems," *IEEE Transactions on Control Systems Technology*, Vol. 5, No. 4, pp. 427-438, 1997.

[14] V.I. Utkin, "Variable structure systems with sliding mode," *IEEE Trans. Auto. Control*, Vol. AC-22, pp. 212-222, 1977.

[15] Z.J. Yang and M. Tateishi, "Adaptive robust nonlinear control of a magnetic levitation system," *Automatica*, Vol. 37, pp. 1125-1131, 2001.

Young Sam Lee

He received his M.Sc degree in Electrical Engineering from Inha University, Inchon, Korea, in 1999. He received his Ph.D. degree in Electrical Engineering from Seoul National University, Seoul, Korea, in 2003. He is currently working as an Associate Professor in the School of Electrical Engineering at Inha University, Inchon, Korea. His research interests are control application, embedded systems, and robotics.

Ji-Hyuk Yang

He received his M.Sc. degree in Electrical Engineering from Inha University, Inchon, Korea, in 2008. He is currently pursuing his Ph.D. degree in Electrical Engineering at Inha University, Inchon, Korea. His primary research interest lies in the development of rapid control prototyping environment.

Su-Yong Shim

He received his B.Sc. degree in Electrical Engineering from Inha University, Inchon, Korea, in 2008. He is currently pursuing his M.Sc. degree in Electrical Engineering at Inha University, Inchon, Korea. His research interests are mechatronics and embedded systems.